



THE UNIVERSITY *of* EDINBURGH

## Edinburgh Research Explorer

# Complementary actions of dopamine D2 receptor 1 agonist and anti-Vegf therapy on tumoral vessel normalization in a transgenic mouse model

### Citation for published version:

Chauvet, N, Romano, N, Lafont, C, Guillou, A, Galibert, E, Bonnefont, X, Le Tissier, P, Fedele, M, Fusco, A, Mollard, P & Coutry, N 2017, 'Complementary actions of dopamine D2 receptor 1 agonist and anti-Vegf therapy on tumoral vessel normalization in a transgenic mouse model', *International Journal of Cancer*.  
<https://doi.org/10.1002/ijc.30628>

### Digital Object Identifier (DOI):

[10.1002/ijc.30628](https://doi.org/10.1002/ijc.30628)

### Link:

[Link to publication record in Edinburgh Research Explorer](#)

### Document Version:

Peer reviewed version

### Published In:

International Journal of Cancer

### Publisher Rights Statement:

This is the author's peer-reviewed manuscript as accepted for publication

### General rights

Copyright for the publications made accessible via the Edinburgh Research Explorer is retained by the author(s) and / or other copyright owners and it is a condition of accessing these publications that users recognise and abide by the legal requirements associated with these rights.

### Take down policy

The University of Edinburgh has made every reasonable effort to ensure that Edinburgh Research Explorer content complies with UK legislation. If you believe that the public display of this file breaches copyright please contact [openaccess@ed.ac.uk](mailto:openaccess@ed.ac.uk) providing details, and we will remove access to the work immediately and investigate your claim.



1 **Title: Complementary actions of dopamine D2 receptor agonist and anti-**  
2 **Vegf therapy on tumoral vessel normalization in a transgenic mouse model**

3

4 **Short Title:** Tumoral vessel normalization by dopamine and Vegf blockade

5

6 **Authors:** Norbert Chauvet<sup>1,2,3,\$</sup>, Nicola Romanò<sup>1,2,3,\$\$</sup>, Chrystel Lafont<sup>1,2,3</sup>, Anne  
7 Guillou<sup>1,2,3</sup>, Evelyne Galibert<sup>1,2,3</sup>, Xavier Bonnefont<sup>1,2,3</sup>, Paul Le Tissier<sup>4</sup>, Monica Fedele<sup>5</sup>,  
8 Alfredo Fusco<sup>5</sup>, Patrice Mollard<sup>1,2,3</sup> and Nathalie Coutry<sup>1,2,3</sup>.

9

10 <sup>1</sup> CNRS, UMR-5203, Institut de Génomique Fonctionnelle, Montpellier, F-34094, France

11 <sup>2</sup> INSERM, U1191, Montpellier, F-34094, France

12 <sup>3</sup> Université de Montpellier, UMR-5203, Montpellier, F-34094, France.

13 <sup>4</sup> Centre for Integrative Physiology, University of Edinburgh, Edinburgh, EH8 9XD, United  
14 Kingdom.

15 <sup>5</sup> Istituto di Endocrinologia ed Oncologia Sperimentale del CNR e/o Dipartimento di  
16 Medicina Molecolare e Biotecnologie Mediche, Università degli Studi di Napoli "Federico  
17 II", 80131 Naples, Italy.

18

19 \$ Present address: PhyMedExp, INSERM U1046, CNRS UMR-9214, Université de  
20 Montpellier, 34295 Montpellier Cedex 5, France.

21 \$\$ Present address: Centre for Integrative Physiology, University of Edinburgh, Edinburgh,  
22 EH8 9XD, United Kingdom.

23

24 **Corresponding author:** Nathalie Coutry, Institut de Génomique Fonctionnelle, 141 rue  
25 de la Cardonille, 34094 Montpellier CEDEX 05, France. Nathalie.Coutry@igf.cnrs.fr.

26

27 **Keywords:** Angiogenesis, mouse model, pituitary adenomas, combination therapy, GPCR  
28 ligand.

29

30 **Abbreviations:** D2R, Dopamine Receptor D2; GPCRs, G Protein-Coupled Receptors; DA,  
31 Dopamine; PRL, Prolactin; WT, Wild-Type; TH, Tyrosine Hydroxylase; pTH,  
32 Phosphorylated Tyrosine Hydroxylase; TEM, Transmission Electron Microscopy; SEM,  
33 Scanning Electron Microscopy; TIDA neurons, TuberoInfundibular Dopamine Neurons.

34

35 **Article Category:** Research Article - Cancer Therapy and Prevention

36

37 **Novelty and Impact:** Angiogenesis in tumors favors many aspects of disease  
38 development and compromises treatment efficiency. The authors aimed to identify a treatment  
39 to normalize tumoral vessels and restore normal blood perfusion with a Vegf receptor  
40 inhibitor and/or a ligand of dopamine G protein-coupled receptor D2. These findings offer a  
41 preclinical proof of concept for a combination therapy that exhibits a robust efficacy to  
42 abrogate intratumoral hemorrhage and restores blood vessel perfusion in a mouse model of  
43 prolactinoma.

44

45 **Financial support:** This work was supported by grants from Institut National de la Santé  
46 et de la Recherche Médicale; Centre National de la Recherche Scientifique; Université de

47 Montpellier; the Agence Nationale de la Recherche (ANR-2010-BLAN-1415-01 and ANR 12  
48 BSV1 0032-01) and the Cancéropôle Grand Sud-Ouest.

49

50 **Conflict of interest:** The authors disclose no potential conflicts of interest.

**51 Abstract**

52 Angiogenesis contributes in multiple ways to disease progression in tumors and reduces  
53 treatment efficiency. Molecular therapies targeting Vegf signaling combined with  
54 chemotherapy or other drugs exhibit promising results to improve efficacy of treatment.  
55 Dopamine has been recently proposed to be a novel safe antiangiogenic drug that stabilizes  
56 abnormal blood vessels and increases therapeutic efficacy. Here, we aimed to identify a  
57 treatment to normalize tumoral vessels and restore normal blood perfusion in tumor tissue  
58 with a Vegf receptor inhibitor and/or a ligand of dopamine G protein-coupled receptor D2  
59 (D2R). Dopamine, via its action on D2R, is an endogenous effector of the pituitary gland, and  
60 we took advantage of this system to address this question. We have used a previously  
61 described Hmga2/T mouse model developing haemorrhagic prolactin-secreting adenomas. In  
62 mutant mice, blood vessels are profoundly altered in tumors, and an aberrant arterial  
63 vascularization develops leading to the loss of dopamine supply. D2R agonist treatment  
64 blocks tumor growth, induces regression of the aberrant blood supply and normalizes blood  
65 vessels. A chronic treatment is able to restore the altered balance between pro- and anti-  
66 angiogenic factors. Remarkably, an acute treatment induces an up-regulation of the stabilizing  
67 factor Angiopoietin 1. An anti-Vegf therapy is also effective to restrain tumor growth and  
68 improves vascular remodeling. Importantly, only the combination treatment suppresses  
69 intratumoral hemorrhage and restores blood vessel perfusion, suggesting that it might  
70 represent an attractive therapy targeting tumor vasculature. Similar strategies targeting other  
71 ligands of GPCRs involved in angiogenesis may identify novel therapeutic opportunities for  
72 cancer.

73

74

75

## 76 **Introduction**

77 Pathological angiogenesis, generated by an imbalance of pro- and antiangiogenic  
78 factors, provides oxygen and nutrients to tumors, and is a hallmark of many benign and  
79 malignant diseases <sup>1,2</sup>. New blood vessels within tumors are impaired in their function and  
80 structure, and this abnormal vascular network causes alterations in blood flow and  
81 oxygenation that can further increase tumor growth and alter the anti-tumor efficiency of  
82 cytotoxic drugs <sup>3,4</sup>. Results from clinical trials using anti-Vegf agents have revealed that  
83 efficacy of anti-angiogenic monotherapy can be inadequate in term of response or survival  
84 rates <sup>5</sup>. To improve treatment efficiency, novel combinations of anti-Vegf therapy with  
85 chemotherapy or radiation have been developed, with promising results <sup>5,6</sup>. Thus, a recent  
86 study performed by Jain's group investigating a combination treatment with anti-Vegf and  
87 chemotherapy, showed that early vessel normalization improves tumor perfusion and survival  
88 in a subset of glioblastoma patients <sup>7</sup>. Of interest, another option is to combine Vegf-signaling  
89 inhibitors with antiangiogenic agents targeting alternative pathways. In this regard, the use of  
90 inhibitors targeting Vegf and Angiopoietin 2 has shown complementary actions on tumor  
91 growth and angiogenesis <sup>8,9</sup>.

92 Alternative strategies for normalizing vessels and blood flow in tumoral tissues are  
93 based on the use of ligands for G protein-coupled receptors (GPCRs) <sup>10</sup>. Among the recently  
94 discovered candidates, D2 receptors and their natural ligand dopamine (DA) are of particular  
95 interest as, in addition to its major role as a neurotransmitter within the brain, DA controls  
96 vascular tone and blocks Vegf-dependent increase in vascular permeability <sup>11,12</sup>. DA  
97 influences tumor behavior as well, especially by controlling cell proliferation and processes  
98 leading to angiogenesis <sup>13,14</sup>. DA is not only an anti-tumoral and anti-angiogenic drug, it also  
99 normalizes abnormal tumor blood vessels by acting on pericytes and endothelial cells, and  
100 therefore improves tumor perfusion by increasing blood flow, decreasing hypoxia and

101 enhancing the concentration of anti-cancer drug in tissue <sup>15</sup>. A recent study showed that DA  
102 therapy also prevents 5-fluoracil mediated neutropenia <sup>16</sup>. Hence, DA has been proposed to be  
103 a novel therapy for the treatment of cancer and chemotherapy-induced disorders <sup>15-17</sup>.

104 In this context, we examined whether an anti-Vegf therapy combined with D2 receptor  
105 ligands could exert additive effects to normalize blood vessels in tumors. We tested this  
106 hypothesis on the pituitary gland since DA is also an endogenous effector of this master gland  
107 and plays a central role in tonically inhibiting prolactin (PRL) release via D2 receptors located  
108 on lactotrophs <sup>18</sup>. Blood perfuses the normal pituitary via incoming vessels from the pituitary  
109 portal circulation at the base of the brain. Previous studies have reported that prolactinomas in  
110 rats <sup>19</sup> and in humans <sup>20</sup> are associated with the development of a direct arterial blood supply,  
111 which may lead in turn to an escape from inhibitory hypothalamic regulation since systemic  
112 blood contains very low DA levels in comparison with portal blood. Prolactinomas are in  
113 general treated by medical therapy with DA agonists, and an anti-angiogenic strategy using  
114 anti-Vegf agents has been recently proposed to treat aggressive human pituitary tumors <sup>21</sup>.  
115 These tumors are therefore an excellent model for investigation of the use of DA and Vegf for  
116 tumor therapy through modification of vascular defects.

117 We have used the Hmga2/T mouse model, which develops PRL-secreting adenomas <sup>22</sup>  
118 and has been previously used to test the efficacy of new drugs for the therapy of human  
119 pituitary tumors <sup>23</sup>, to investigate the status of endogenous DA during tumoral development  
120 and the effects of a D2R agonist on tumor growth and vasculature. Moreover, we have  
121 examined whether DA and anti-Vegf agent could exert complementary effects on structural  
122 and functional properties of tumoral blood vessels. We show that a loss in endogenous DA  
123 inhibitory tone is concomitant with tumor progression and is associated with aberrant growth  
124 of blood vessels. D2R agonist treatment inhibits tumor growth and normalizes abnormal  
125 blood vessels. Molecular mechanisms induced by D2R agonist are able to reverse the

126 profound alterations of the angiogenic profile in tumoral glands and involve an up-regulation  
127 of the stabilizing factor Angiopoietin1. Strikingly, although anti-Vegf treatment is also able to  
128 normalize tumoral blood vessels and prevents tumor growth, only the combination treatment  
129 suppresses intratumoral hemorrhage and restores blood vessel perfusion.

130

## 131 **Materials and Methods**

### 132 **Mouse model**

133 All animal studies complied with the animal welfare guidelines of the European  
134 Community. They were approved by the Direction of Veterinary departments of Hérault and  
135 the Languedoc Roussillon Institutional Animal Care and Use Committee (#CEEA-LR-  
136 12119). Animals were housed in light (12-hour light, 12-hour dark cycle) and temperature  
137 (22-24°C) controlled rooms and fed a normal diet with free access to tap water.

138 Experiments were performed on mixed 129/SVJ x C57BL/6 female mice, either wild-  
139 type (WT) or overexpressing ubiquitously a truncated form of Hmga2 protein<sup>24</sup> (Hmga2/T  
140 mice). In this model, pituitaries from females exhibited an extended period of hyperplasia,  
141 starting around 3 months of age, followed by tumor onset between 9 to 11 months  
142 (Supporting Information Fig. 1). These tumors appeared very hemorrhagic and  
143 immunohistochemical experiments showed that they were prolactinomas. A strong correlation  
144 was observed between circulating PRL levels and tumor weight ( $R^2 = 0.936$ ), as reported in  
145 human prolactinomas<sup>25,26</sup>. We thus decided to monitor hormone output for each mouse once  
146 a week to follow tumor initiation and progression. Unless otherwise specified, the majority of  
147 experiments were performed on cohorts of mice with circulating PRL concentrations between  
148 400 and 800 ng/ml and corresponding to tumors of 13-18 mg.

149

### 150 **ELISA assay for PRL**



151 Blood levels of PRL were measured using an ultra-sensitive ELISA method recently  
152 established in the laboratory<sup>27</sup>. Briefly, whole blood (4  $\mu$ l) was collected from the tail vein of  
153 conscious mice, immediately diluted (1/30) in PBS-T (PBS, 0.05% Tween20), and then  
154 frozen at  $-20^{\circ}\text{C}$  until use.

155

### 156 **Injection or administration of drugs in mice**

157 The dopaminergic inhibitory tone was evaluated by an intraperitoneal (ip) injection of  
158 the D2R antagonist domperidone (20 mg/kg, Abcam) and measurement of circulating PRL 3  
159 times before (basal) and then 30 min and 45 min after the injection. The DA inhibitory tone  
160 was determined by the maximum fold increase in PRL blood levels and corresponds to the  
161 ratio between the maximum secretion and the basal level (mean of PRL blood concentration  
162 of the 3 points preceding domperidone injection).

163 Bromocriptine mesylate implants (60 days, 10 mg pellet, Innovative Research of  
164 America) were placed under the skin of the neck of Hmga2/T mice harboring pituitary  
165 tumors, for 6 weeks. Some mice received ip injections of bromocriptine (6 mg/kg, Sigma-  
166 Aldrich) twice a day over the course of 48 h.

167 Axitinib (20 mg/kg, Abmole Bioscience Inc.) or sucralose were given to the mice by  
168 voluntary oral administration, twice a day for 6 weeks, after training of the mice  
169 (<http://www.nature.com/protocolexchange/protocols/2099>).

170

### 171 **Immunohistochemistry**

172 Immunohistochemical analyses were performed as previously reported<sup>28</sup>. Briefly,  
173 pituitary tissue sections from WT and Hmga2/T mice with and without various treatments  
174 were prepared with a vibratome and then stained with a sheep polyclonal tyrosine  
175 hydroxylase antibody (TH, 1:1000, Ab113, Abcam), with a rabbit polyclonal phosphorylated

176 TH antibody (pTH, 1:1000, AB5423, Milipore), or with a rat monoclonal endomucin antibody  
177 (1:500, sc-53941, Santa Cruz) as a marker for pituitary endothelial cells. In one set of  
178 experiments, pituitary paraffin sections were stained with a rat monoclonal endomucin  
179 antibody (1:500, sc-53941, Santa Cruz). Sections were observed with an epifluorescence  
180 (Carl-Zeiss Axio Imager Z1) or a confocal microscope (LSM510 Zeiss). Four parameters  
181 were evaluated using ImageJ software to characterize quantitatively pituitary  
182 microvasculature: the mean vessel area, the microvessel density, the total vessel area and the  
183 area of extravasation of red blood cells. Detailed protocol is presented in Supporting  
184 Information Material and Method section.

185

#### 186 **Scanning and Transmission Electron Microscopy**

187 Ultrastructural analyses were performed as previously described <sup>29</sup>, in WT and  
188 Hmga2/T mice receiving or not different treatments. Different parameters characterizing  
189 blood vessel structure observed by Transmission Electron Microscopy (TEM) were quantified  
190 using ImageJ software: the perimeter of the lumen, the circularity (a value of 1 indicates a  
191 perfect circle) and the solidity (defined as the ratio of an object area/area of the convex hull of  
192 the object, objects with irregular shapes have a solidity value approaching 0), reflecting the  
193 tortuosity of the vessels.

194

#### 195 **Injection of microspheres in the general circulation**

196 To assess vascular supply in pituitary adenomas, fluorescent microsphere were  
197 injected in the circulation following a previously described protocol <sup>19</sup>. Minor modifications  
198 are presented in Supporting Information Material and Methods section.

199

#### 200 ***In vivo* amperometry**

201 A detailed protocol of *in vivo* amperometry is given in Supporting Information  
202 Material and Methods section. Briefly, after anaesthesia with ketamine-xylazine, mice were  
203 fixed on a stereotactic frame, and a carbon fiber microelectrode was inserted in a support  
204 guide cannula, with its tip reaching the median eminence at stereotaxic coordinates -1.3 mm  
205 rostro-caudal; 0 mm medio-lateral; 6.1 mm ventral. After at least one week of recovery, mice  
206 were transferred to the recording cages and connected to an electrical swivel to enable free  
207 movement. The microelectrodes were maintained at 700 mV to detect secretion of DA, and  
208 oxidation currents were recorded at 1 kHz.

209

#### 210 ***In vivo* imaging of pituitary gland**

211 Cellular *in vivo* imaging of the pituitary gland allows determination of microvascular  
212 organisation and blood flow in the same region of the gland, and a detailed protocol has been  
213 previously reported <sup>30</sup>. Injections of 150 kDa FITC-labeled dextran (Sigma-Aldrich) were  
214 performed via the jugular vein in WT and Hmga2/T mice. Fluorescence emission was  
215 captured by an EM-CCD camera 512 x 512 C9100 (Hamamatsu) and acquired with  
216 MetaMorph software (Molecular Devices).

217

#### 218 **Blood vessel perfusion**

219 WT or Hmga2/T mice were anesthetized by inhalation of isoflurane (1.5% in O<sub>2</sub>) and  
220 a catheter was inserted in the jugular vein. Perfusion of blood vessels was evaluated after an  
221 intravenous injection of 1 mg of fluorescent 500 kDa dextran (dextran fluorescein, lysine  
222 fixable, Molecular Probes). After circulation for 15 min, a thoracic lethal dose of  
223 pentobarbital was administrated to the mice and pituitaries were fixed in 4% PFA. Tissue  
224 sections were prepared using a vibratome, and blood vessels were immunostained using an

225 endomucin antibody. Volocity software was used to measure overlap coefficient (M1)  
226 according to Manders et al.<sup>31</sup> reflecting the portion of blood vessels filled with dextran.

227

### 228 **Real-time RT-PCR**

229 Adenohypophysis were dissected from terminally anaesthetized mice. Total RNA was  
230 extracted and then reverse-transcribed as previously described<sup>28,32</sup>. Specific primers for qRT-  
231 PCR were designed using the Primer Express 3.0 software, the sequences are shown in  
232 Supporting Information Table 1. PCR reactions are presented in Supporting Information  
233 Material and Method section.

234

### 235 **Statistics**

236 Values represent mean  $\pm$  SEM. Statistical tests were performed with Prism (GraphPad  
237 software). Normality was assessed using D'Agostino-Pearson test. Non-parametric statistical  
238 tests were used for some data sets, as indicated in figure legends. Multiple comparisons tests  
239 were selected when the number of data sets were  $>2$ . Statistical difference between groups  
240 was assumed when  $P < 0.05$ .

241

## 242 **Results**

### 243 **Aberrant blood supply leads to loss of dopaminergic inhibitory tone, associated with** 244 **tumor progression**

245 We first characterized the vascular network in pituitary tumors by  
246 immunohistochemistry, scanning electron microscopy (SEM) and TEM (Fig. 1). The results  
247 demonstrate remodeling of the microvasculature in the tumors and structural abnormalities.  
248 The vascular density was decreased in tumors compared to WT, and tumoral blood vessels  
249 were dilated, tortuous and structurally altered (Fig. 1A and B) since blood lakes were present

250 (Fig. 1B and J). Changes in the organization of the vascular architecture in tumors were also  
251 confirmed at the ultrastructural level (Fig. 1 C to J). The endothelium of the blood vessels was  
252 irregular, discontinuous and damaged, presenting numerous protrusions into the lumen of the  
253 vessels, as described for other tumor types<sup>33</sup>.

254 To test whether tumorigenesis in our model was associated with the development of a  
255 direct arterial blood supply, we injected in the systemic circulation fluorescent microspheres  
256 with a diameter which is too large to pass through the primary portal capillaries in the median  
257 eminence (Supporting Information Fig. 2). Whilst in WT animals microspheres were  
258 restricted to the median eminence (Supporting Information Fig. 2A and B), in mice harboring  
259 tumors microspheres were also localized in the tumoral region (Supporting Information Fig.  
260 2C and D). The development of such an aberrant growth of blood vessels in tumors was  
261 directly visualized by *in vivo* imaging of the pituitary after an intravenous injection of  
262 fluorescent dextran. In WT mice (Fig. 1K), as expected, blood flow arrived from the median  
263 eminence through the portal system, and filled capillaries from the entire gland in a rostro-  
264 caudal direction in less than 30 s. Although arteries from meninges surrounding pituitary were  
265 rapidly filled ( $t = 2$  s), they never branched with the adenohypophysis blood vessels. By  
266 contrast, in *Hmga2/T* mice with a tumor beginning to develop (Fig. 1L), the blood flow from  
267 the portal system in the hyperplastic area was strongly slowed, while the tumoral region was  
268 perfused by vessels derived from dural arteries (Fig. 1L, arrow heads).

269 The development of this aberrant direct vascularization induced a loss of endogenous  
270 DA inhibitory tone, although DA was still produced and released by tuberoinfundibular  
271 dopamine (TIDA) neurons (Fig. 2). By determining circulating PRL after an injection of a  
272 D2R antagonist, domperidone, in WT and hyperplastic glands, we found that the endogenous  
273 DA inhibitory tone was high (Fig. 2A). By contrast, it was decreased in 7-20 mg tumors, and  
274 very low, albeit still present, in tumors  $\geq 20$  mg. In addition, phosphorylated tyrosine

275 hydroxylase (the key enzyme involved in DA synthesis) was still present in neurons from the  
276 arcuate nucleus from *Hmga2/T* mice with pituitary tumors (Fig. 2B), suggesting that DA was  
277 produced in TIDA neurons. Accordingly, DA was released *in vivo* by TIDA neurons in the  
278 median eminence where it normally diffuses into the capillaries of the pituitary portal blood  
279 vessels. We performed *in vivo* amperometric measurements of DA secretion (Fig. 2C).  
280 Episodic secretion of DA was still detectable in animals with pituitary tumors, and did not  
281 appear grossly different from that in WT animals (Nicola Romanò, personal communication).  
282 Furthermore, the frequency of amperometric events did not decrease during tumor  
283 development (Fig 2C).

284 Overall, these findings show that establishment of an aberrant blood supply leads to the  
285 loss in DA inhibitory tone, secondary to tumor onset, without major hypothalamic  
286 dysfunction.

287

### 288 **D2R agonist blocks aberrant blood supply, tumor progression and restores angiogenic** 289 **balance**

290 To evaluate the impact of restoring DA on blood supply, we treated mice harboring  
291 pituitary tumors (Tumors t0), with subcutaneous implants of a D2R agonist bromocriptine for  
292 6 weeks (Bromocriptine 6 wks), and then analyzed the presence of the aberrant growth of  
293 blood vessels (Fig. 3). Of note, bromocriptine was able to inhibit PRL secretion: 24 hours  
294 after the implantation circulating PRL concentrations were low and remained controlled until  
295 sacrifice (< 50 ng/ml, data not shown), indicating that the *Hmga2/T* model had the ability to  
296 respond to bromocriptine treatment. This treatment totally blocked tumoral growth compared  
297 to untreated tumors (Tumors 6 wks, Fig. 3B). Pituitary weight was similar to that measured in  
298 Tumors t0 (Fig. 3B), and pituitaries appeared less hemorrhagic (Fig. 3A). Strikingly,  
299 bromocriptine treatment inhibited the progression of the aberrant vascularization as revealed

300 by a drastic decrease in the number of microspheres in pituitaries from bromocriptine-treated  
301 animals compared to untreated mice (Fig. 3C). The 5-fold decrease in the number of  
302 microspheres quantified between Tumors t0 and bromocriptine-treated tumors suggests that  
303 the D2R agonist induced a partial regression of the pre-existing aberrant vascularization.  
304 Immunostaining for D2R showed that D2R was present as expected in lactotrophs, but it was  
305 also detected in pituitary blood vessels (Supporting Information Fig. 3), suggesting that DA  
306 could exert its effects directly on blood vessels.

307 We then investigated whether this chronic D2R agonist treatment could affect the  
308 expression of a panel of pro- and anti-angiogenic factors. Fig. 3D shows that the angiogenic  
309 profile, assessed by qPCR, was affected in tumors: angiogenic factor expression was up- or  
310 down-regulated, whilst during the period of hyperplasia, modulations were modest  
311 (Supporting Information Fig. 4A). Interestingly, bromocriptine treatment for 6 weeks was  
312 able to reverse these alterations (Fig. 3E) and restored an angiogenic signature close to that  
313 observed during hyperplasia (Supporting Information Fig. 4B).

314 We next assessed the kinetics of bromocriptine action on the angiogenic gene expression  
315 profile. After 2 days of treatment, among the set of genes studied, only 2 were rapidly  
316 regulated by bromocriptine (Fig. 3F; Supporting Information Fig. 4C): *angiopoietin 1*  
317 (*Angpt1*) and *Prok1* (also named EG-Vegf) an angiogenic mitogen specific to endocrine  
318 glands<sup>34</sup>. The mRNA levels for *Angpt1* were low in tumors and an acute bromocriptine  
319 treatment restored its expression totally since the mRNA levels were similar to that found in  
320 WT animals (relative expression for *Angpt1*:  $2.37 \pm 0.32$  in WT vs  $2.41 \pm 0.47$  in  
321 bromocriptine-treated mice). *Prok1* expression was partially restored by an acute  
322 bromocriptine treatment: relative expression for *Prok1* was  $1.68 \pm 0.13$  and  $0.98 \pm 0.46$  in  
323 WT and bromocriptine-treated mice, respectively. *Vegfa* expression was not affected by  
324 bromocriptine treatment. Altogether, these results show that the D2R agonist blocked tumor

325 growth, induced regression of the aberrant vascularization and up-regulated the expression of  
326 *Angpt1* and *Prok1*.

327

### 328 **Vegf contributes both to aberrant blood supply and tumoral growth**

329 Vegf has been shown to be involved in normal and tumoral vascular remodeling<sup>5,35</sup> and  
330 has been reported to contribute to pituitary tumor progression in a murine model<sup>36</sup>. We  
331 investigated whether Vegf could participate in the occurrence and development of the  
332 aberrant vascularization in tumors. We first established that aberrant direct vascularization  
333 starts to develop in mice with circulating PRL between 75 and 100 ng/ml (data not shown).  
334 We treated mice exhibiting such concentrations of PRL for 6 weeks with axitinib, a potent  
335 inhibitor of tyrosine kinase and selective from VegfR<sup>37</sup>. Axitinib-treated tumors appeared  
336 less hemorrhagic than control tumors (Fig. 4A) and the antiangiogenic agent partially blocked  
337 tumor progression (Fig. 4B). The number of microspheres quantified in axitinib-treated  
338 tumors was significantly lower than in those of controls, demonstrating that Vegf contributes  
339 to the establishment of the aberrant blood supply in tumors (Fig. 4C). The effects of axitinib  
340 on expression of pro- and anti-angiogenic factors (Fig. 4D) showed that the angiogenic gene  
341 profile was differentially affected by axitinib compared to bromocriptine treatment (Fig. 3E),  
342 although some genes were regulated in a similar way by both treatments such as *Rgs5* and  
343 *Cspg4* for example. Importantly, the expression of *Angpt1* and *Prok1*, which was up-regulated  
344 in response to bromocriptine treatment, was unchanged and remained low after axitinib  
345 treatment (Fig. 4D). These results suggest that D2R agonist treatment and anti-Vegf therapy  
346 could involve common as well as independent effects on angiogenic pathways.

347

348 **Bromocriptine or axitinib correct the structural abnormalities of tumoral vessels while**  
349 **the combination treatment restores blood vessel perfusion**



350 We further addressed the complementary effects of D2R agonist and anti-Vegf therapy  
351 on blood vessel normalization (Fig. 5 and Supporting Information Fig. 5). Figure 5A shows  
352 that the combination treatment greatly reduced intratumoral hemorrhage. Analysis of pituitary  
353 vasculature in various conditions and morphometric measurements of blood vessels  
354 demonstrate that D2R agonist or axitinib had an equivalent capacity to improve structural  
355 defects present in tumoral blood vessels and that the combination treatment did not lead to a  
356 significant advantage (Fig. 5B and C and Supporting Information Fig. 5). Whilst vascular  
357 density was maintained in presence of D2R agonist treatment compared to untreated-tumors,  
358 axitinib notably decreased vascular density. In addition, blood vessel dilatation and tortuosity  
359 were improved by the different treatments (Supporting Information Fig. 5).

360 Leakiness of tumoral blood vessels is of particular functional significance and  
361 intratumoral hemorrhage constitutes an indicator of this leakiness<sup>33</sup>. Importantly, the  
362 combination treatment dramatically reduced leakiness of blood vessels (Fig. 5D).  
363 Quantification of the area of extravasation in various conditions showed that intratumoral  
364 hemorrhage in tumors represented more than 7% of the total surface area. Although it was  
365 significantly reduced by both bromocriptine or axitinib, only the combination treatment was  
366 able to prevent vessel leakiness since intratumoral hemorrhage was almost absent in  
367 bromocriptine + axitinib-treated tumors.

368 Because of the highly disorganized epithelium lining endothelial cells, blood vessel  
369 perfusion is severely impaired in tumors<sup>38</sup>. We assessed whether the positive effects of the  
370 combination treatment also included an improved vessel perfusion (Fig. 6). The portion of  
371 blood vessels filled with FITC-dextran was significantly decreased in tumors compared to  
372 WT (Fig. 6A and B), indicating that perfusion within the tumors was strongly affected and  
373 inappropriate. Bromocriptine- and axitinib-treatment improved partially vessel perfusion, and  
374 the combination treatment restored this almost entirely. Together, these results show that,

375 whilst bromocriptine and/or axitinib were able to correct structural abnormalities of tumoral  
376 vessels with a similar efficacy, only the combination treatment restored their function.

377

## 378 **Discussion**

379 We report here that a combination of D2R agonist treatment with anti-Vegf therapy  
380 specifically suppresses intratumoral hemorrhage and restores the perfusion of blood vessels.  
381 PRL-secreting pituitary adenomas undergo profound vascular remodeling along with  
382 formation of an aberrant arterial blood supply resulting in an escape from inhibitory  
383 hypothalamic regulation by DA. D2R agonist treatment blocks tumor growth and remarkably  
384 ameliorates abnormal blood vessel function. In addition, the altered balance between pro- and  
385 anti-angiogenic factors in tumors is restored by D2R agonist administration. An anti-Vegf  
386 therapy is also able to inhibit tumor growth and improves vascular remodeling. Furthermore,  
387 we show for the first time that a combination of anti-Vegf and GPCR ligand therapy exerts  
388 complementary effects on tumoral blood vessel normalization.

389 *Dual effects of dopamine on angiogenesis process.* We show, in accordance with  
390 previous studies<sup>35,36</sup>, that anti-Vegf therapy induced a drastic reduction in vascular density.  
391 This anti-angiogenic effect was effective both on capillaries of the portal system and the  
392 extra-portal aberrant vascularization. By contrast, D2R agonist effects specifically induced the  
393 regression of the extra-portal aberrant vascularization. These antiangiogenic effects might be  
394 mediated in part via DA action on Vegf signaling<sup>11,39,40</sup>. Notably, both treatments strongly  
395 down-regulated the angiogenic factor Rgs5, whose expression is closely associated with  
396 tumor-induced neovascularization and drastically reduced in vessels normalized under  
397 therapy<sup>41</sup>. Despite the regression of this extra-portal blood system, the maintenance of the  
398 vascular density in D2R agonist-treated tumors may be due to the formation of *de novo*  
399 capillaries derived from the portal system, suggesting that DA could exert dual effects on

400 vascularization. Endothelial cells display a strong heterogeneity in terms of structure, function  
401 or gene expression<sup>42</sup>. It is now well established that in tumors endothelial cells show multiple  
402 phenotypes that can vary during tumor progression and are mainly determined by the  
403 microenvironment<sup>43</sup>. It is possible that D2R agonists act on both the extraportal and the portal  
404 blood system by distinct mechanisms, and these effects are probably mediated via different  
405 combinations of effectors. In this respect, Prok1 (also named EG-Vegf) is an interesting  
406 candidate to mediate specific DA actions. In humans, Prok1 has been shown to have a highly  
407 tissue-specific pattern of expression, and was proposed to be a mitogen that could regulate  
408 tissue-specific proliferation and differentiation of endothelial cells<sup>34</sup>, in particular in  
409 endocrine glands. We show that its expression is down-regulated in prolactinomas and rapidly  
410 restored by D2R agonist treatment. Thus, this angiogenic factor could play a role in DA-  
411 induced vasculature remodeling, especially in the formation of *de novo* blood vessels from the  
412 portal system.

413 ***Vascular normalization by D2R agonist and Vegf inhibition.*** Although anti-Vegf  
414 specific monotherapy may not be as effective as initially expected in term of response and  
415 increase survival in patients with cancers, its combination with modulation of other signaling  
416 pathways may have promise<sup>5,6</sup>. We show that anti-Vegf and D2R agonist treatments given  
417 alone displayed partial and similar efficiency on blood vessel perfusion and intratumoral  
418 hemorrhage. Remarkably, D2R agonist and blockade of Vegf together had additive effects on  
419 vascular perfusion and leakage, suggesting complementary modes of action. This is supported  
420 by analysis of angiogenic factors rapidly regulated by DA, which highlighted Angpt1 as a  
421 putative candidate normalizing blood vessels. Up-regulation of Angpt1 was also maintained  
422 during long term D2R agonist treatment, while after anti-Vegf monotherapy Angpt1 levels  
423 remained low. Angpt1 and 2 are ligands of the vascular endothelial Tie2 receptor and bind to  
424 Tie2 with similar affinities, however they behave as mutual antagonists<sup>44</sup>. Therefore, the

425 balance of Angpt1 and Angpt2 is critical for control of vascular normalization or angiogenesis  
426 via the same Tie2 receptor <sup>45</sup>. Of note, in the present study, the Angpt1/Angpt2 ratio was  
427 decreased in tumors, and this ratio was reversed with the administration of D2R agonists.  
428 Vegf and Angpt1 exert antagonist effects on endothelial barrier function since Vegf increases  
429 vascular permeability, an effect which is inhibited by Angpt1, which also promotes blood  
430 vessels stabilization <sup>44</sup>. Recent studies show that targeted Angpt1 monotherapy in pathological  
431 conditions is highly effective to suppress vascular leakage <sup>46,47</sup>. Moreover, DA-normalization  
432 of blood vessels in murine orthotopic models of colon and prostate cancers involved up-  
433 regulation of Angpt1 <sup>15</sup>. We show here that DA effects on Vegf signaling is not sufficient to  
434 abrogate vascular leakage and concomitant Vegf blockade is required to totally suppress  
435 intratumoral hemorrhage.

436 In summary, the present study demonstrates that D2R agonist and anti-Vegf therapy  
437 exert complementary actions on tumoral vessel normalization. This combinatorial approach  
438 might constitute an interesting option in treatment of prolactinomas, especially in cases where  
439 current therapy is ineffective or poorly tolerated. We anticipate that the novel combination  
440 treatment proposed in the present study could treat different tumor types in which DA exerts  
441 anti-angiogenic effects or normalizes tumoral blood vessels, such as ovarian carcinoma, lung  
442 cancer or colon cancer <sup>15, 16, 48, 49</sup>. Growing evidence implicates GPCRs and their downstream  
443 signaling pathways in cancer pathology, especially angiogenesis <sup>50</sup>. Since the GPCRs are  
444 excellent drug targets, a similar combinatorial strategy extending to different ligands of  
445 GPCRs involved in angiogenesis may identify novel therapeutic opportunities for cancer.

446

#### 447 **Acknowledgments**

448 The authors would like to thank J. Guillemin and F. Gallardo from animal facility of Institute  
449 for Functional Genomics for their assistance with the transgenic mouse lines, and are grateful

450 to S. Debiesse for genotyping service. Dr A. O. Martin is gratefully acknowledged for helpful  
451 discussions on the project, Dr P. de Santa Barbara for critical reading of the manuscript, and  
452 P. Fontanaud for technical assistance with imaging analysis. The authors thank Dr C.  
453 Cazevielle for assistance with the electron microscope (Montpellier RIO Imaging-INM-  
454 COMET).

455

#### 456 **Statement of author contributions**

457

458 NC, NR, CL and NC conceived, designed and carried out experiments. Data were analysed  
459 and interpreted by NC, NR, CL and NC. NC and NC supervised the project. AG and EG  
460 carried out experiments. MF and AF provided the Hmga2/T mouse model. NC, NR, XB, PLT,  
461 PM and NC were involved in writing the manuscript. All authors had final approval of the  
462 manuscript.

463

#### 464 **References**

465 1. Carmeliet P, Jain RK. Molecular mechanisms and clinical applications of  
466 angiogenesis. *Nature* 2011;473:298-307.

467 2. Goel S, Duda DG, Xu L, Munn LL, Boucher Y, Fukumura D, Jain RK.  
468 Normalization of the vasculature for treatment of cancer and other diseases. *Physiol Rev*  
469 2011;91:1071-121.

470 3. Hanahan D, Folkman J. Patterns and emerging mechanisms of the angiogenic  
471 switch during tumorigenesis. *Cell* 1996;86:353-64.

472 4. Jain RK. Normalization of tumor vasculature: an emerging concept in  
473 antiangiogenic therapy. *Science (New York, N.Y.)* 2005;307:58-62.

474 5. Jain RK, Duda DG, Clark JW, Loeffler JS. Lessons from phase III clinical trials on  
475 anti-VEGF therapy for cancer. *Nat Clin Prac Oncol* 2006;3:24-40.

476 6. Jayson GC, Kerbel R, Ellis LM, Harris AL. Antiangiogenic therapy in oncology:  
477 current status and future directions. *Lancet* 2016.

478 7. Batchelor TT, Gerstner ER, Emblem KE, Duda DG, Kalpathy-Cramer J, Snuderl M,  
479 Ancukiewicz M, Polaskova P, Pinho MC, Jennings D, Plotkin SR, Chi AS, et al. Improved  
480 tumor oxygenation and survival in glioblastoma patients who show increased blood perfusion  
481 after cediranib and chemoradiation. *Proc Natl Acad Sci USA* 2013;110:19059-64.

482 8. Hashizume H, Falcon BL, Kuroda T, Baluk P, Coxon A, Yu D, Bready JV, Oliner  
483 JD, McDonald DM. Complementary Actions of Inhibitors of Angiopoietin-2 and VEGF on  
484 Tumor Angiogenesis and Growth. *Cancer Res* 2010;70:2213-23.

485 9. Peterson TE, Kirkpatrick ND, Huang YH, Farrar CT, Marijt KA, Kloepper J, Datta  
486 M, Amoozgar Z, Seano G, Jung K, Kamoun WS, Vardam T, et al. Dual inhibition of Ang-2

- 487 and VEGF receptors normalizes tumor vasculature and prolongs survival in glioblastoma by  
488 altering macrophages. *Proc Natl Acad Sci USA* 2016;113:4470-75.
- 489 10. Lappano R, Maggiolini M. G protein-coupled receptors: novel targets for drug  
490 discovery in cancer. *Nat Rev Drug Discov* 2011;10:47-60.
- 491 11. Basu S, Nagy JA, Pal S, Vasile E, Eckelhoefer IA, Bliss VS, Manseau EJ,  
492 Dasgupta PS, Dvorak HF, Mukhopadhyay D. The neurotransmitter dopamine inhibits  
493 angiogenesis induced by vascular permeability factor/vascular endothelial growth factor. *Nat*  
494 *Med* 2001;7:569-74.
- 495 12. Bhattacharya R, Sinha S, Yang SP, Patra C, Dutta S, Wang E, Mukhopadhyay D.  
496 The neurotransmitter dopamine modulates vascular permeability in the endothelium. *J Mol*  
497 *Signal* 2008;3:14.
- 498 13. Sarkar C, Chakroborty D, Basu S. Neurotransmitters as regulators of tumor  
499 angiogenesis and immunity: the role of catecholamines. *J Neuroimmune Pharmacol* 2013;8:7-  
500 14.
- 501 14. Peters MA, Walenkamp AM, Kema IP, Meijer C, de Vries EG, Oosting SF.  
502 Dopamine and serotonin regulate tumor behavior by affecting angiogenesis. *Drug Resist*  
503 *Updat* 2014;17:96-104.
- 504 15. Chakroborty D, Sarkar C, Yu H, Wang J, Liu Z, Dasgupta PS, Basu S. Dopamine  
505 stabilizes tumor blood vessels by up-regulating angiopoietin 1 expression in pericytes and  
506 Kruppel-like factor-2 expression in tumor endothelial cells. *Proc Natl Acad Sci USA*  
507 2011;108:20730-5.
- 508 16. Sarkar C, Chakroborty D, Dasgupta PS, Basu S. Dopamine is a safe antiangiogenic  
509 drug which can also prevent 5-fluorouracil induced neutropenia. *Int J Cancer* 2015;137:744-9.
- 510 17. Banerjee SK. Dopamine: an old target in a new therapy. *J Cell Commun Signal*  
511 2015;9:85-6.
- 512 18. Grattan DR, Kokay IC. Prolactin: a pleiotropic neuroendocrine hormone. *J*  
513 *Neuroendocrinol* 2008;20:752-63.
- 514 19. Elias KA, Weiner RI. Direct arterial vascularization of estrogen-induced prolactin-  
515 secreting anterior pituitary tumors. *Proc Natl Acad Sci USA* 1984;81:4549-53.
- 516 20. Schechter J, Goldsmith P, Wilson C, Weiner R. Morphological evidence for the  
517 presence of arteries in human prolactinomas. *J Clin Endocrinol Metab* 1988;67:713-9.
- 518 21. Ortiz LD, Syro LV, Scheithauer BW, Ersen A, Uribe H, Fadul CE, Rotondo F,  
519 Horvath E, Kovacs K. Anti-VEGF therapy in pituitary carcinoma. *Pituitary* 2012;15:445-9.
- 520 22. Fedele M, Battista S, Kenyon L, Baldassarre G, Fidanza V, Klein-Szanto AJP,  
521 Parlow AF, Visone R, Pierantoni GM, Outwater E, Santoro M, Croce CM, et al.  
522 Overexpression of the HMGA2 gene in transgenic mice leads to the onset of pituitary  
523 adenomas. *Oncogene* 2002;21:3190-98.
- 524 23. Fedele M, De Martino I, Pivonello R, Ciarmiello A, De Caro MLDB, Visone R,  
525 Palmieri D, Pierantoni GM, Arra C, Schmid HA, Hofland L, Lombardi G, et al. SOM230, a  
526 new somatostatin analogue, is highly effective in the therapy of growth hormone/prolactin-  
527 secreting pituitary adenomas. *Clin Cancer Res* 2007;13:2738-44.
- 528 24. Battista S, Fidanza V, Fedele M, Klein-Szanto AJ, Outwater E, Brunner H,  
529 Santoro M, Croce CM, Fusco A. The expression of a truncated HMGI-C gene induces  
530 gigantism associated with lipomatosis. *Cancer Res* 1999;59:4793-7.
- 531 25. Delgrange E, Trouillas J, Maiter D, Donckier J, Tourniaire J. Sex-related  
532 difference in the growth of prolactinomas: a clinical and proliferation marker study. *J Clin*  
533 *Endocrinol Metab* 1997;82:2102-7.
- 534 26. Losa M, Mortini P, Barzaghi R, Gioia L, Giovanelli M. Surgical treatment of  
535 prolactin-secreting pituitary adenomas: early results and long-term outcome. *J Clin*  
536 *Endocrinol Metab* 2002;87:3180-6.

- 537 27. Guillou A, Romano N, Steyn F, Abitbol K, Le Tissier P, Bonnefont X, Chen C,  
538 Mollard P, Martin AO. Assessment of lactotroph axis functionality in mice: longitudinal  
539 monitoring of PRL secretion by ultrasensitive-ELISA. *Endocrinology* 2015;156:1924-30.
- 540 28. Chauvet N, El-Yandouzi T, Mathieu MN, Schlernitzauer A, Galibert E, Lafont C,  
541 Le Tissier P, Robinson IC, Mollard P, Coutry N. Characterization of adherens junction  
542 protein expression and localization in pituitary cell networks. *J Endocrinol* 2009;202:375-87.
- 543 29. Bonnefont X, Lacampagne A, Sanchez-Hormigo A, Fino E, Creff A, Mathieu MN,  
544 Smallwood S, Carmignac D, Fontanaud P, Travo P, Alonso G, Courtois-Coutry N, et al.  
545 Revealing the large-scale network organization of growth hormone-secreting cells. *Proc Natl*  
546 *Acad Sci USA* 2005;102:16880-5.
- 547 30. Lafont C, Desarmenien MG, Cassou M, Molino F, Lecoq J, Hodson D,  
548 Lacampagne A, Mennessier G, El Yandouzi T, Carmignac D, Fontanaud P, Christian H, et al.  
549 Cellular in vivo imaging reveals coordinated regulation of pituitary microcirculation and GH  
550 cell network function. *Proc Natl Acad Sci USA* 2010;107:4465-70.
- 551 31. Manders EMM, Verbeek FJ, Aten JA. MEASUREMENT OF  
552 COLOCALIZATION OF OBJECTS IN DUAL-COLOR CONFOCAL IMAGES. *J*  
553 *Microscopy* 1993;169:375-82.
- 554 32. Osterstock G, El Yandouzi T, Romano N, Carmignac D, Langlet F, Coutry N,  
555 Guillou A, Schaeffer M, Chauvet N, Vanacker C, Galibert E, Dehouck B, et al. Sustained  
556 alterations of hypothalamic tanycytes during posttraumatic hypopituitarism in male mice.  
557 *Endocrinology* 2014;155:1887-98.
- 558 33. Hashizume H, Baluk P, Morikawa S, McLean JW, Thurston G, Roberge S, Jain  
559 RK, McDonald DM. Openings between defective endothelial cells explain tumor vessel  
560 leakiness. *Am J Pathol* 2000;156:1363-80.
- 561 34. LeCouter J, Kowalski J, Foster J, Hass P, Zhang Z, Dillard-Telm L, Frantz G,  
562 Rangell L, DeGuzman L, Keller GA, Peale F, Gurney A, et al. Identification of an angiogenic  
563 mitogen selective for endocrine gland endothelium. *Nature* 2001;412:877-84.
- 564 35. Kamba T, Tam BYY, Hashizume H, Haskell A, Sennino B, Mancuso MR,  
565 Norberg SM, O'Brien SM, Davis RB, Gowen LC, Anderson KD, Thurston G, et al. VEGF-  
566 dependent plasticity of fenestrated capillaries in the normal adult microvasculature. *Am J*  
567 *Physiol Heart Circ Physiol* 2006;290:H560-H76.
- 568 36. Korsisaari N, Ross J, Wu X, Kowanetz M, Pal N, Hall L, Eastham-Anderson J,  
569 Forrest WF, Van Bruggen N, Peale FV, Ferrara N. Blocking vascular endothelial growth  
570 factor-A inhibits the growth of pituitary adenomas and lowers serum prolactin level in a  
571 mouse model of multiple endocrine neoplasia type 1. *Clin Cancer Res* 2008;14:249-58.
- 572 37. Hu-Lowe DD, Zou HY, Grazzini ML, Hallin ME, Wickman GR, Amundson K,  
573 Chen JH, Rewolinski DA, Yamazaki S, Wu EY, McTigue MA, Murray BW, et al.  
574 Nonclinical antiangiogenesis and antitumor activities of axitinib (AG-013736), an oral,  
575 potent, and selective inhibitor of vascular endothelial growth factor receptor tyrosine kinases  
576 1, 2, 3. *Clin Cancer Res* 2008;14:7272-83.
- 577 38. Carmeliet P, Jain RK. Principles and mechanisms of vessel normalization for  
578 cancer and other angiogenic diseases. *Nat Rev Drug Discov* 2011;10:417-27.
- 579 39. Chakroborty D, Sarkar C, Mitra RB, Banerjee S, Dasgupta PS, Basu S. Depleted  
580 dopamine in gastric cancer tissues: dopamine treatment retards growth of gastric cancer by  
581 inhibiting angiogenesis. *Clin Cancer Res* 2004;10:4349-56.
- 582 40. Cristina C, Luque GM, Demarchi G, Lopez Vicchi F, Zubeldia-Brenner L, Perez  
583 Millan MI, Perrone S, Ornstein AM, Lacau-Mengido IM, Berner SI, Becu-Villalobos D.  
584 Angiogenesis in pituitary adenomas: human studies and new mutant mouse models. *Int J*  
585 *Endocrinol* 2014;2014:608497.

- 586 41. Berger M, Bergers G, Arnold B, Hammerling GJ, Ganss R. Regulator of G-protein  
587 signaling-5 induction in pericytes coincides with active vessel remodeling during  
588 neovascularization. *Blood* 2005;105:1094-101.
- 589 42. Aird WC. Endothelial cell heterogeneity. *Cold Spring Harb Perspect Med*  
590 2012;2:a006429.
- 591 43. Hida K, Ohga N, Akiyama K, Maishi N, Hida Y. Heterogeneity of tumor  
592 endothelial cells. *Cancer Sci* 2013;104:1391-5.
- 593 44. Augustin HG, Koh GY, Thurston G, Alitalo K. Control of vascular morphogenesis  
594 and homeostasis through the angiopoietin-Tie system. *Nat Rev Mol Cell Biol* 2009;10:165-  
595 77.
- 596 45. Saharinen P, Eklund L, Pulkki K, Bono P, Alitalo K. VEGF and angiopoietin  
597 signaling in tumor angiogenesis and metastasis. *Trends Mol Med* 2011;17:347-62.
- 598 46. Dessapt-Baradez C, Woolf AS, White KE, Pan J, Huang JL, Hayward AA, Price  
599 KL, Kolatsi-Joannou M, Locatelli M, Diennet M, Webster Z, Smillie SJ, et al. Targeted  
600 Glomerular Angiopoietin-1 Therapy for Early Diabetic Kidney Disease. *J Am Soc Nephrol*  
601 2014;25:33-42.
- 602 47. Lee J, Park D-Y, Park DY, Park I, Chang W, Nakaoka Y, Komuro I, Yoo O-J,  
603 Koh GY. Angiopoietin-1 Suppresses Choroidal Neovascularization and Vascular Leakage.  
604 *Invest Ophthalmol Vis Sci* 2014;55:2191-99.
- 605 48. Moreno-Smith M, Lee SJ, Lu C, Nagaraja AS, He G, Rupaimoole R, Han HD,  
606 Jennings NB, Roh JW, Nishimura M, Kang Y, Allen JK, et al. Biologic effects of dopamine  
607 on tumor vasculature in ovarian carcinoma. *Neoplasia* 2013;15:502-10.
- 608 49. Hoepfner LH, Wang Y, Sharma A, Javeed N, Van Keulen VP, Wang E, Yang P,  
609 Roden AC, Peikert T, Molina JR, Mukhopadhyay D. Dopamine D2 receptor agonists inhibit  
610 lung cancer progression by reducing angiogenesis and tumor infiltrating myeloid derived  
611 suppressor cells. *Mol Onc* 2015;9:270-81.
- 612 50. O'Hayre M, Degese MS, Gutkind JS. Novel insights into G protein and G protein-  
613 coupled receptor signaling in cancer. *Curr Opin Cell Biol* 2014;27:126-35.
- 614  
615

## 616 **Figure Legends**

### 617 **Figure 1: Aberrant growth of blood vessels in Hmga2/T tumors.**

618 (A and B) Representative sections of pituitary from WT (A) and pituitary tumors from  
619 Hmga2/T (B) mice immunostained with endomucin, a marker of blood vessels. Vascular  
620 density was lower in tumors and tumoral blood vessels were structurally altered, exhibiting  
621 dilation and strong tortuosity (arrows). Extravasation of red blood cells was present in tumors  
622 (double arrows). Scale bar: 50  $\mu$ m. (C-G) Blood vessels visualized by SEM in pituitary  
623 sections from WT (C) and Hmga2/T mice (D-G). Vessels were enlarged and disorganized in  
624 tumors (D and F). Endothelial cells in tumor vessels overlapped one another with abnormal  
625 connections (E, arrows). (G) Higher magnification of F showing endothelial cells protruding



626 into the lumen (asterisk). Scale bar: 5  $\mu\text{m}$  in C; 10  $\mu\text{m}$  in D-G. (H-J) Ultrastructural  
627 visualization of blood vessels by transmission electron microscopy in pituitary from WT (H)  
628 and Hmga2/T mice (I and J). A capillary from normal pituitary, surrounded by endocrine  
629 cells, displayed a regular and smooth endothelium, a perivascular space with collagen fibers.  
630 By contrast, in tumors, vessels were large and disorganized. The endothelium was damaged,  
631 protrusions into the lumen were observed (arrows, I), and numerous red blood cells were  
632 present outside the vessels (asterisks, I and J). Scale bar: 5  $\mu\text{m}$  in H-J. (K and L) *In vivo*  
633 imaging of pituitaries from WT (K) and Hmga2/T (L) mice after iv injection of fluorescent  
634 labeled-dextran. In WT, fluorescence was first detected in dural arteries from meninges  
635 surrounding the pituitary (arrows). Fluorescence was present in the adenohypophysis after 4 s  
636 and the whole pituitary vasculature was filled after 24 s. In Hmga2/T mice, in the tumoral  
637 region, the fluorescence was observed in vessels derived from dural arteries (arrowheads).  
638 Note that detection of fluorescence in the adenohypophysis through the portal system started  
639 at 21 s. Filling of the portal capillaries was complete after 1 min and 49 s. Letters C and R  
640 indicate the caudal-rostral orientation of the animal.

641

642 **Figure 2: The direct arterial blood supply in tumors impedes the dopaminergic**  
643 **inhibitory tone without major hypothalamic dysfunction.**

644 (A) Dopaminergic inhibitory tone in WT and Hmga2/T mice at various stages. PRL blood  
645 concentrations were measured in basal conditions and after an injection of the D2R antagonist  
646 domperidone. The DA inhibitory tone (ratio between maximal and basal PRL secretion  $\pm$   
647 sem) was high in wild-type mice and during hyperplasia while tumors displayed a  
648 significantly lower tone. WT: n = 7; Hyperplasia: n = 7; Tumors 7-20 mg: n = 6; Tumors  
649 >20mg: n = 8. (B) Confocal images showing immunofluorescence labeling of hypothalamus  
650 sections from WT (left) and Hmga2/T mice (right) with TH (top) and phosphorylated TH

651 (pTH, bottom) antibodies. The staining obtained with TH or pTH antibody was similar in the  
652 arcuate nucleus and median eminence region in WT and Hmga2/T mice, showing that TIDA  
653 neurons were present and still produced DA in animals harboring tumors. Scale bar: 100  $\mu$ m.

654 (C) Amperometric measurements of DA secretion in the median eminence *in vivo* before the  
655 onset of tumors and during tumoral progression assessed by PRL concentration in blood.

656

657 **Figure 3: Bromocriptine prevents tumoral progression, aberrant vascular supply, and**  
658 **restores angiogenic balance.**

659 (A) Photographs of pituitary adenomas from Hmga2/T mice with (Bromocriptine 6 wks) and  
660 without (Tumor 6 wks) treatment with bromocriptine implants for 6 weeks, compared to  
661 pituitary tumor at the beginning of the treatment (Tumor t0). Scale bar: 2 mm. (B) Weight of  
662 pituitaries from Hmga2/T mice at the beginning of the treatment (Tumors t0, n = 6), or  
663 receiving or not (Tumors 6 wks, n = 6) bromocriptine for 6 weeks (Bromocriptine 6 wks, n =  
664 5). Tumoral progression was inhibited by bromocriptine. Kruskal-Wallis test followed by  
665 Dunn's multiple comparisons test, \*\* P<0.01. (C) Quantification of microspheres present in  
666 the adenohipophysis of Hmga2/T mice at the beginning of the treatment, or receiving or not  
667 bromocriptine for 6 weeks. The number of microspheres was significantly lower in  
668 bromocriptine-treated mice (n = 5) compared to untreated mice (n = 6). Kruskal-Wallis test  
669 followed by Dunn's multiple comparisons test, \*\*\* P<0.001. (D) Expression of pro- and anti-  
670 angiogenic factors in tumoral Hmga2/T compared to WT mice. Angiogenic factor mRNA  
671 levels were quantified in Hmga2/T mice harboring pituitary tumors (n = 7) and WT of similar  
672 age (n = 5) by qPCR. Angiogenic profiles were altered in pituitary adenomas. Mann-Whitney  
673 test, \* P<0.05, \*\* P<0.01. (E) Long-term effects of bromocriptine on angiogenic profiles in  
674 pituitary tumors. Angiogenic factor mRNA levels were quantified by qPCR in Hmga2/T mice  
675 harboring pituitary tumors and treated (n = 4) or not (n = 7) with implants of bromocriptine

676 for 6 weeks. Results are presented as ratio of gene expression in bromocriptine-treated tumors  
677 to untreated-tumors and show that bromocriptine restored the expression of angiogenic factors  
678 in tumors. Mann-Whitney test, \*  $P < 0.05$ , \*\*  $P < 0.01$ . (F) *Angpt1*, *Prokl* and *Vegfa* mRNA  
679 expression in pituitaries from *Hmga2/T* mice harboring tumors that received an acute  
680 treatment with bromocriptine (n = 5) or vehicle (n = 5). While *Vegfa* expression was not  
681 modified by bromocriptine, the D2R agonist increased *Angpt1* and *Prokl* mRNA levels.  
682 Mann-Whitney test, \*  $P < 0.05$ .

683

684 **Figure 4: Involvement of Vegf in the establishment of aberrant blood supply and tumor**  
685 **growth.**

686 (A) Photographs of pituitary adenomas from *Hmga2/T* mice treated after tumor onset for 6  
687 weeks with vehicle or the anti-angiogenic agent axitinib. Axitinib-treated tumors appeared  
688 less hemorrhagic and tumor growth was reduced. (B) Weight of pituitaries from *Hmga2/T*  
689 mice receiving vehicle or axitinib for 6 weeks. Tumoral growth was decreased by axitinib.  
690 Mann Whitney test, \*\*  $P < 0.01$ . (C) Quantification of microspheres present in the  
691 adenohypophysis from *Hmga2/T* mice receiving vehicle or axitinib for 6 weeks. The number  
692 of microspheres was significantly lower in axitinib-treated mice (n = 5) compared to vehicle-  
693 treated mice (n = 6). Mann Whitney test, \*\*  $P < 0.01$ . (D) Long-term effects of axitinib on  
694 angiogenic profiles in pituitary tumors. Angiogenic factor mRNA levels were quantified by  
695 qPCR in *Hmga2/T* mice harboring pituitary tumors and treated (n = 4) or not (n = 6) with  
696 axitinib for 6 weeks. Results are presented as ratio of gene expression in axitinib-treated  
697 tumors to untreated-tumors and show that axitinib did not restore the expression of *Angpt1*  
698 and *Prokl* in tumors. Mann-Whitney test, \*  $P < 0.05$ , \*\*  $P < 0.01$ .

699

700 **Figure 5: Complementary effects of bromocriptine and axitinib on intratumoral**  
701 **hemorrhage.**

702 (A) Photographs of pituitary adenomas from Hmga2/T mice harboring untreated-tumors, or  
703 tumors treated for 6 weeks with either bromocriptine or axitinib, or combined bromocriptine  
704 and axitinib. (B) Paraffin embedded pituitary sections from WT mice, hyperplastic Hmga2/T  
705 mice, and Hmga2/T mice with pituitary tumors receiving various treatments for 6 weeks.  
706 Tissue sections were immunostained with endomucin, a marker of blood vessels. Scale bar:  
707 50  $\mu\text{m}$ . Arrows: blood lakes. To better illustrate vascular density and defects, corresponding  
708 binary images obtained for quantification of blood vessel structural parameters are shown. (C)  
709 Ultra-structural visualization of pituitary blood vessels by TEM from WT and Hmga2/T mice  
710 exhibiting untreated-tumors, or tumors treated for 6 weeks with various therapies. Scale bar: 5  
711  $\mu\text{m}$ . (D) Quantification of extravasation area in pituitary sections from WT and Hmga2/T  
712 mice receiving various treatments. Combination treatment with bromocriptine and axitinib  
713 almost totally abolished intratumoral hemorrhage.  $n = 4$  mice per condition. Kruskal-Wallis  
714 test followed by Dunn's multiple comparisons test, \*  $P < 0.05$ , \*\*  $P < 0.01$ , \*\*\*  $P < 0.001$ .

715

716 **Figure 6: Restoration of blood vessel perfusion by bromocriptine and axitinib**  
717 **combination treatment.**

718 (A) Blood vessel perfusion was assessed by intravenous injection of FITC-dextran in WT and  
719 Hmga2/T mice receiving various treatments. Pituitary sections were stained with endomucin  
720 (red) to visualize microvasculature. Poorly perfused blood vessels appeared in red and are  
721 particularly numerous in images obtained from untreated tumors. By contrast, the majority of  
722 blood vessels from tumors treated with both bromocriptine and axitinib exhibited green  
723 fluorescence. Scale bar: 200  $\mu\text{m}$ . (B) Quantification of the overlap coefficient M1 reflecting  
724 the fraction of blood vessels filled with FITC-dextran in WT and Hmga2/T mice.

725 Combination treatment with bromocriptine and axitinib restored blood vessel perfusion,  
726 which was strongly impaired in untreated tumors, more effectively than each therapy alone. n  
727 = 4 mice per condition. Kruskal-Wallis test followed by Dunn's multiple comparisons test,  
728 \*\*\* P<0.001.  
729  
730

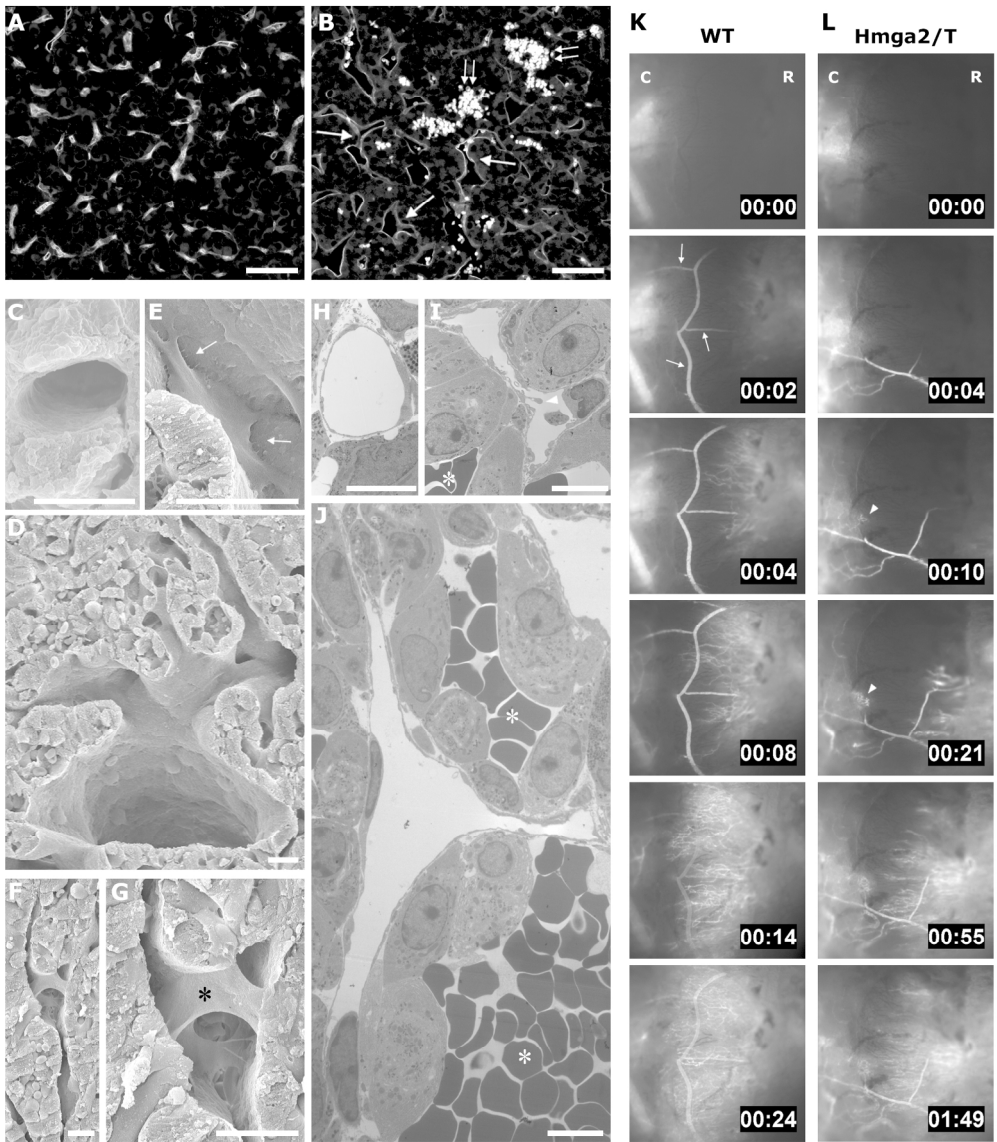


Figure 1: Aberrant growth of blood vessels in Hmga2/T tumors.  
Figure 1  
184x213mm (300 x 300 DPI)

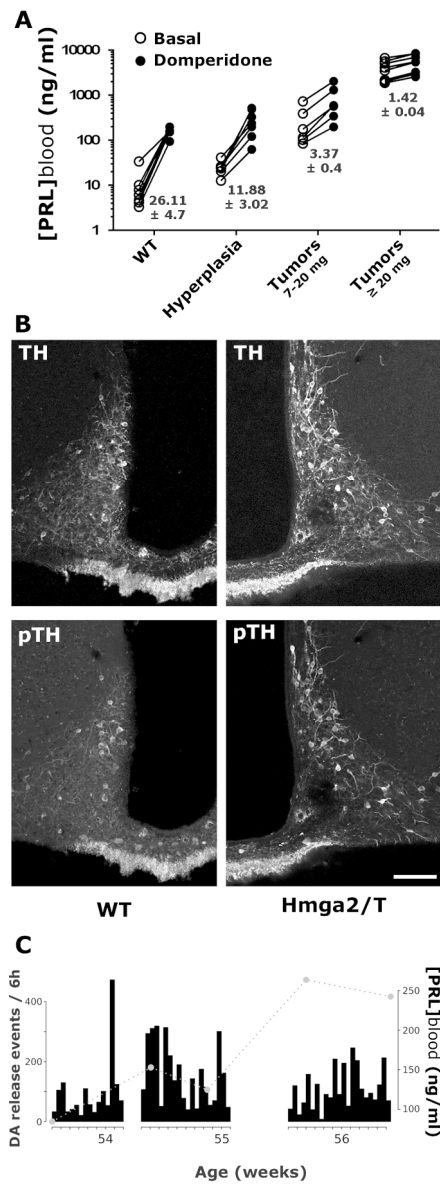


Figure 2: The direct arterial blood supply in tumors impedes the dopaminergic inhibitory tone without major hypothalamic dysfunction.

Figure 2  
79x214mm (300 x 300 DPI)

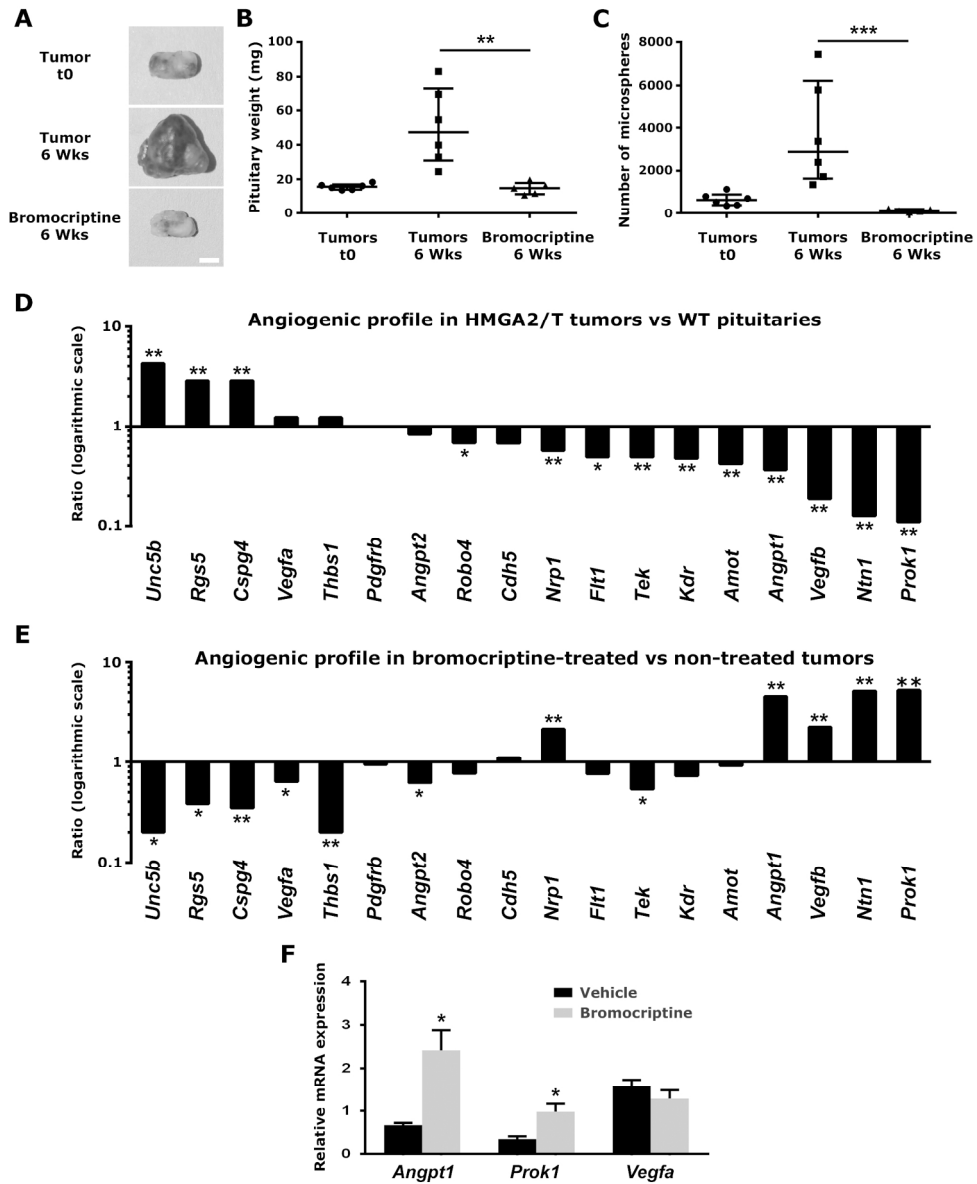


Figure 3: Bromocriptine prevents tumoral progression, aberrant vascular supply, and restores angiogenic balance.

Figure 3

170x209mm (300 x 300 DPI)



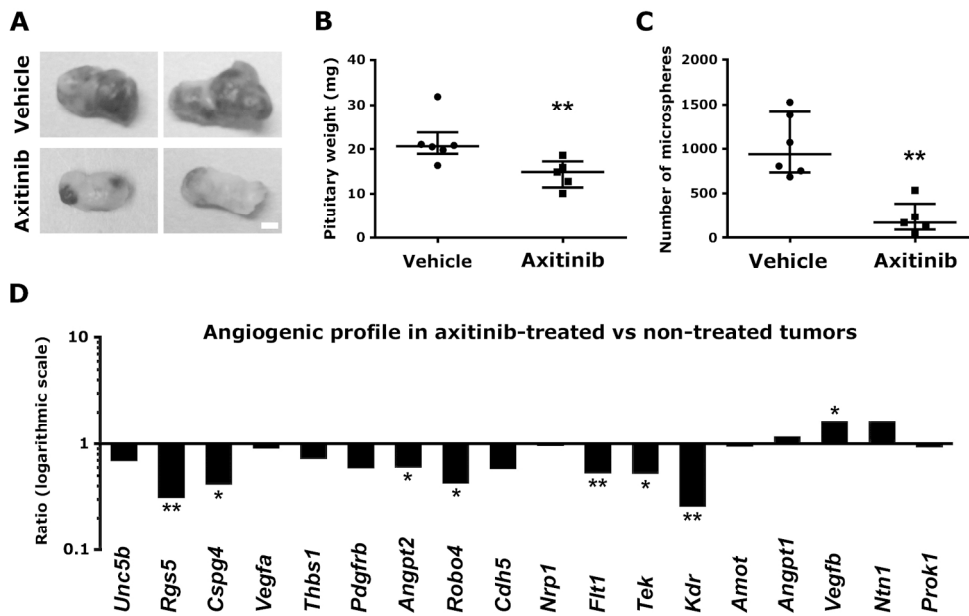


Figure 4: Involvement of Vegf in the establishment of aberrant blood supply and tumor growth.

Figure 4

163x102mm (300 x 300 DPI)

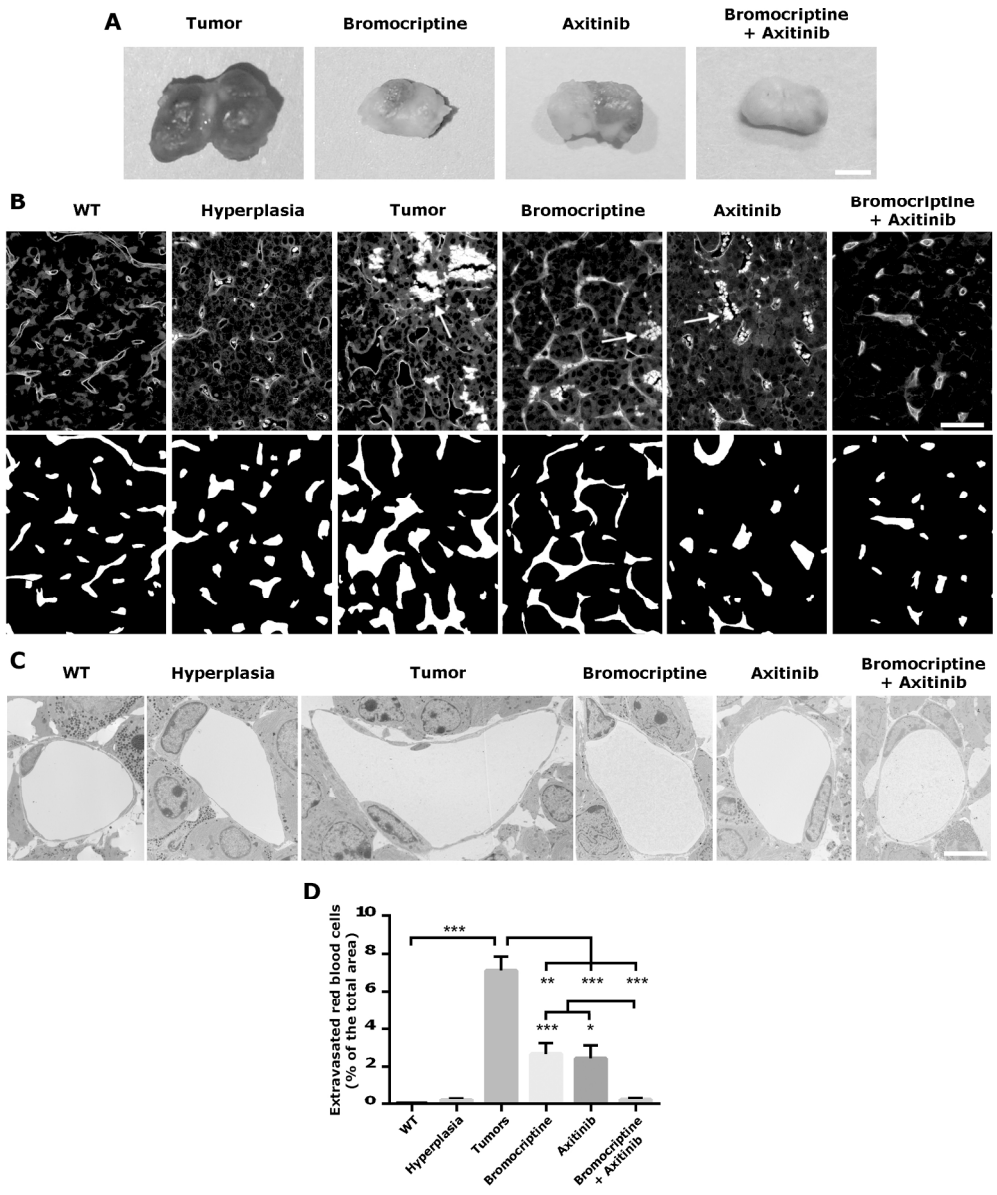


Figure 5: Complementary effects of bromocriptine and axitinib on intratumoral hemorrhage.  
Figure 5  
184x222mm (300 x 300 DPI)

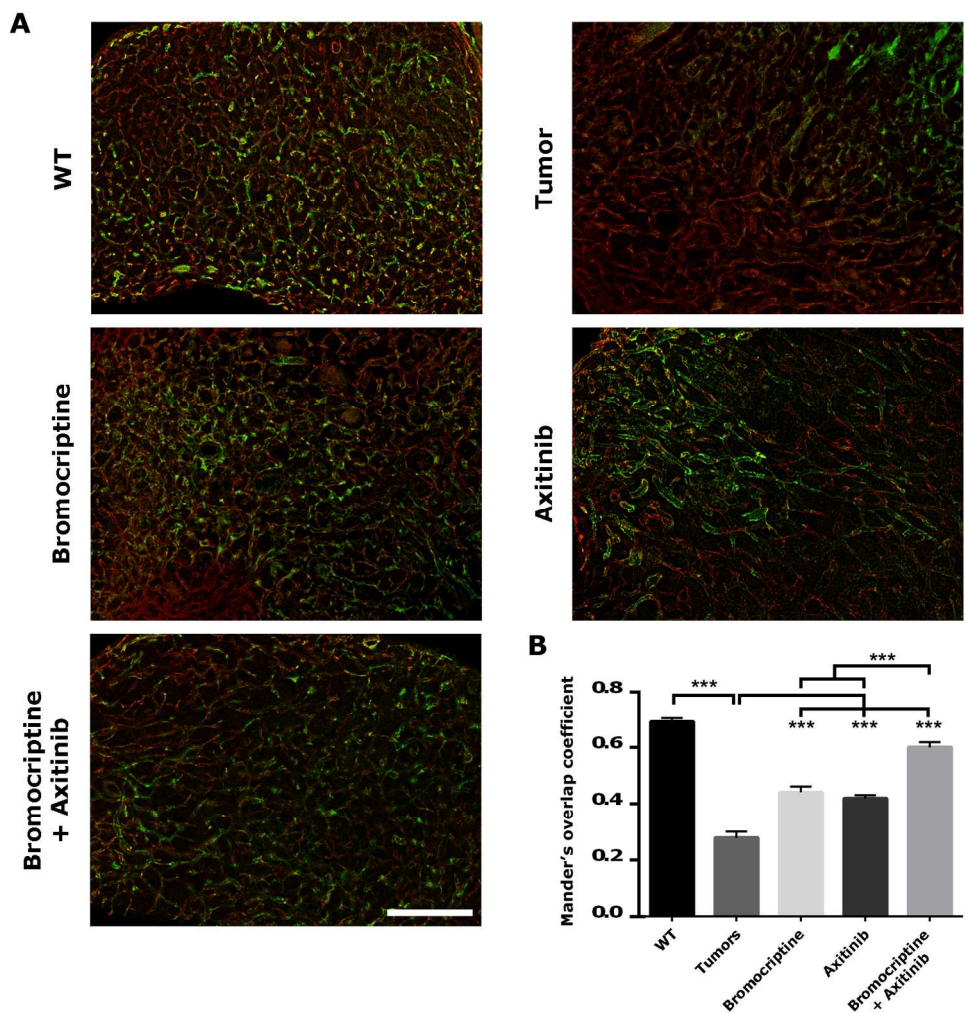


Figure 6: Restoration of blood vessel perfusion by bromocriptine and axitinib combination treatment.

Figure 6

156x159mm (300 x 300 DPI)